Available online at www.sciencedirect.com

ScienceDirect

Scripta Materialia 106 (2015) 30–33

Scripta MATERIALIA

www.elsevier.com/locate/scriptamat

Out-of-plane auxeticity in sintered fibre network mats

Suresh Neelakantan,[a] Jin-Chong Tan[b] and Athina E. Markaki[a,*]

[a]*Department of Engineering, University of Cambridge, Trumpington Street, Cambridge CB2 1PZ, UK*
[b]*Department of Engineering Science, University of Oxford, Parks Road, Oxford OX1 3PJ, UK*

Received 30 March 2015; accepted 19 April 2015
Available online 15 May 2015

Fibre network mats composed of stainless steel exhibit an unusually large out-of-plane auxeticity (i.e. high negative Poisson's ratio v) when subjected to in-plane tensile loading. *In situ* observations in a scanning electron microscope suggest that this is attributable to fibre segment straightening. An investigation was carried out on the effects of fibre volume fraction and network thickness on the auxetic response. Weak inter-layer bonding, high fibre content and low network thickness were found to amplify the auxetic effect.

Keywords: Porous material; Fibres; Tension test; Stainless steels; Poisson's ratio

Conventional materials contract laterally when stretched along their length. By contrast, auxetic materials exhibit a dilatational behaviour, i.e. they expand in the transverse direction when stretched, and are therefore characterised by negative values of Poisson's ratio ($v = -$transverse strain/axial strain) [1–3]. Auxetic materials are of interest due to their potential to achieve enhancement of material properties related to Poisson's ratio [1,4–7]. For 3D isotropic materials, the numerical limits for Poisson's ratio v are set by -1 and 0.5, arising from the relationship between the Poisson's ratio, the bulk K and shear G moduli [6,8]. However, for anisotropic materials, these are independent elastic constants, so strong auxetic effects are theoretically permissible. A schematic showing the wide range of negative Poisson's ratios measured experimentally for various materials is illustrated in Figure 1. Low auxeticity naturally exists in some single crystals (e.g. sulfide minerals, metals, metalloids and intermetallics) [8–12]. Similar levels of auxeticity have been observed in silicates (α-cristobalite, zeolites) attributed to rotation of "building blocks" [13,14]; cubic metals when stretched in [1 1 0] direction [11]; liquid crystalline polymers (e.g. carbocyclic-, poly(phenylacetylene)-networks) due to the connectivity between the rigid centre region and the flexible ends of elongated organic molecules [2,15–17] and skin tissue (cat, cow teat) attributed to their fibrillar structure [18,19]. Man-made auxetic materials include re-entrant or hinged honeycombs and foams, which exhibit auxeticity due to the unfolding of re-entrant cells [1,20–23]; microporous polymers (Polytetrafluoroethylene (PTFE), ultra-high molecular weight polyethylene (UHMWPE), Polypropylene (PP)) [2,24,25]. These polymers consist of an interconnected network of nodules and fibrils and auxeticity has been attributed to the fibrils causing nodule translation when a load is applied [2,25–27]. Auxetic effects have also been observed in fibre composites involving the use of auxetic constituents (polymeric or ceramic fibres [28,29]) or selection of suitable stacking sequences of unidirectional laminae [30–33]. However, high levels of auxeticity in fibre composites have only been achieved by the incorporation of metallic fibre networks [29]. These networks can be used as a stand-alone material [34] or as reinforcement in composites [29]. Such fibre assemblies are highly oriented (fibres oriented mostly in-plane) and are produced by sintering fibres together at crossover points. They are in many respects intermediate between "materials" and "structures".

The measured out-of-plane Poisson's ratios of metallic fibre network mats [29,34–36] reported to date are summarised in Table 1. Values as negative as -18 have been reported. However, the reason for such a large auxeticity has so far not been demonstrated experimentally. This study aims to elucidate the mechanism that causes such a large out-of-plane auxeticity in fibre networks. Herein the effects of fibre volume fraction and mat thickness on the out-of-plane Poisson's ratio have been investigated.

Fibre network plates, made of 316L austenitic stainless steel (N.V. Bekaert S.A., Belgium), were supplied in three different fibre volume fractions f (10, 15 and 20 vol.%) and three thicknesses, t (1, 2 and 5 mm). The 316L fibres are produced by a bundle drawing process and have a hexagonal cross-sectional shape (diagonal length 40 μm). Network plates, made of 444 ferritic stainless steel fibres (Nikko Techno, Japan), have also been considered in this study. The plates are 5 mm thick and contain 15 vol.% of rectangular (80×100 μm^2) 444 fibres, produced by a coil-shaving process. The network plates are processed as follows [35–37]: (i) overlapping of individual slender fibres to form fibre webs of fixed density with random planar orientation;

* Corresponding author.

http://dx.doi.org/10.1016/j.scriptamat.2015.04.028
1359-6462/

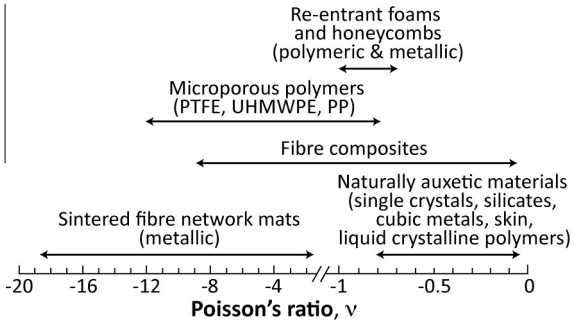

Figure 1. Schematic showing the range of negative Poisson's ratio in auxetic materials.

(ii) stacking few layers of such fibre webs upon one another, compressed and sintered to plates of specific dimensions.

In situ tensile testing of 316L fibre networks was carried out using a Zeiss Evo LS15 VP model scanning electron microscope in secondary electron mode. A DEBEN® tensile stage, equipped with a 5 kN load cell, was mounted in the SEM stage. Rectangular dog-bone tensile specimens were electro-discharge machined from 316L network plates according to ASTM E8-11 sub-size specimen standards. The gauge sections were 30 mm long (x direction), 6 mm wide (y direction) and 5 mm thick (z direction). In order to prevent crushing in the grip sections, the ends of the specimens were impregnated by Loctite super glue. To increase the chances of capturing the auxetic mechanism *in situ*, a further region within the sample gauge section, was impregnated with Loctite super glue thereby leaving roughly 9 mm exposure region to the electron beam. All tests were conducted in displacement control mode at a rate of 0.1 mm min^{-1}. The cross-head displacement was measured using an LVDT.

In-plane tensile testing was carried using an Instron testing machine fitted with a 5 kN load cell. Rectangular dog-bone samples were cut out from 316L network plates of different thicknesses (1, 2, 5 mm) and 5 mm thick 444 networks. The in-plane dimensions of the sample gauge sections were identical to those used for *in situ* tensile testing. The displacements in the xz plane were captured using Digital Image Correlation (DIC) and analysed in order to evaluate the out-of-plane Poisson's ratios as described elsewhere [34].

A Dynamic Mechanical Analyser (DMA, Triton Technology Ltd) was used to measure the out-of-plane Young's modulus (E_z) of the 316L fibre networks with different fibre volume fractions. The tests were carried out in three-point bending mode, with a 12.5 mm loading span, at 1 Hz frequency and 0.1 mm displacement amplitude. Network beams, measuring 5 mm in thickness and 6 mm in width, were used.

For all experiments (except the *in situ* experiment where a single sample was used), at least 3 tests were carried out for each sample type, from which the average value was taken and standard deviation calculated.

For *in situ* tensile testing, the through-thickness face (xz plane) of the 316L networks was exposed to the electron gun. A region within the sample gauge section, as shown in Figure 2, was identified to continuously monitor *in situ*, while applying an in-plane tensile load on the sample. Figure 2a shows the through-thickness view, with fibres (highlighted in red) appearing inwardly bent. During in-plane loading (0.4% strain), the bent fibres (highlighted in red) were found to straighten up as illustrated in Figure 2b. This is also evident from the video (*click on the video link (only for online version) showing the behaviour*), suggesting that fibre straightening or outward bending causes lateral expansion of the sample in the through-thickness direction. The corollary is that, during processing, the through-thickness pressure causes the fibre segments between joints to curve inwards. When the networks are stretched in-plane, the fibres straighten or bend outwards. *In situ* observations suggest that the fibre segments with high radius of curvature (a few mm) are the ones that straightened up compared to those with low radius of curvature.

In our previous study [34], the out-of-plane Poisson's ratios were found to become more negative as the fibre volume fraction increases. Figure 3a shows the longitudinal strain ε_x as a function of the out-of-plane strain ε_z of 316L networks with three fibre volume fractions. Given that during sintering the applied compression pressure increases with fibre volume fraction, it can be postulated that fibres at high density networks protrude more inwards during processing compared with the low density ones resulting in a larger lateral expansion in response to axial (in-plane) loading. This is in agreement with previously measured mean fibre segment inclination angles [34] obtained from X-ray tomography.

Table 1. Negative out-of-plane Poisson's ratio values measured for transversely isotropic metallic fibre networks subjected to in-plane tension. In all studies the fibre material was austenitic stainless steel 316L supplied by N.V. Bekaert, Belgium.

Network thickness t (mm)	Fibre diameter (μm)	Fibre volume fraction f (%)	Out-of-plane Poisson's ratio $-\nu_{xz}$ (−)	Method for strain measurement	Reference
10	12	20	1.7	Clip-gauge extensometer	[35]
Unknown	30	20–40	5.4–18.6	Laser extensometer	[29]
5	40	10–20	5.3–10.7	Digital Image Correlation	[34]

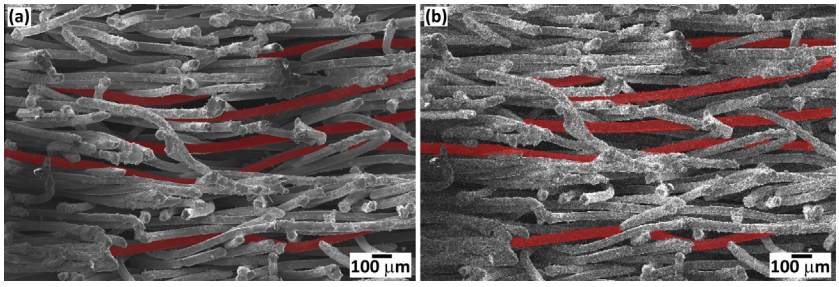

Figure 2. Scanning electron microscopy images of a region in the through-thickness face of the 316L fibre networks ($f = 10\%$) showing fibres (some of them highlighted in red) (a) before and (b) after application of an in-plane tensile load (applied horizontally) corresponding to 0.4% strain. (For interpretation of the references to colour in this figure legend, the reader is referred to the web version of this article.)

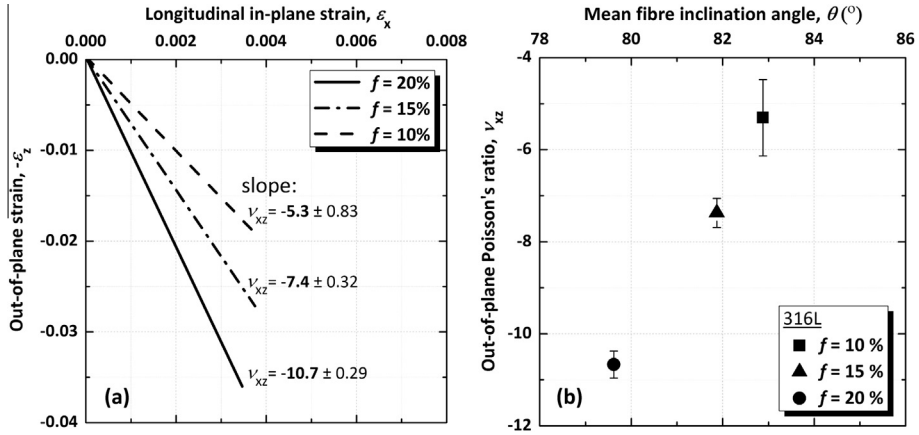

Figure 3. (a) In-plane longitudinal strain as a function of out-of-plane strain, measured during in-plane tensile testing of 316L fibre networks, for three different fibre volume fractions [34]; (b) out-of-plane Poisson's ratio plotted as a function of mean fibre inclination angles (with respect to the through-thickness direction), obtained from X-ray tomography, for different fibre volume fractions [34].

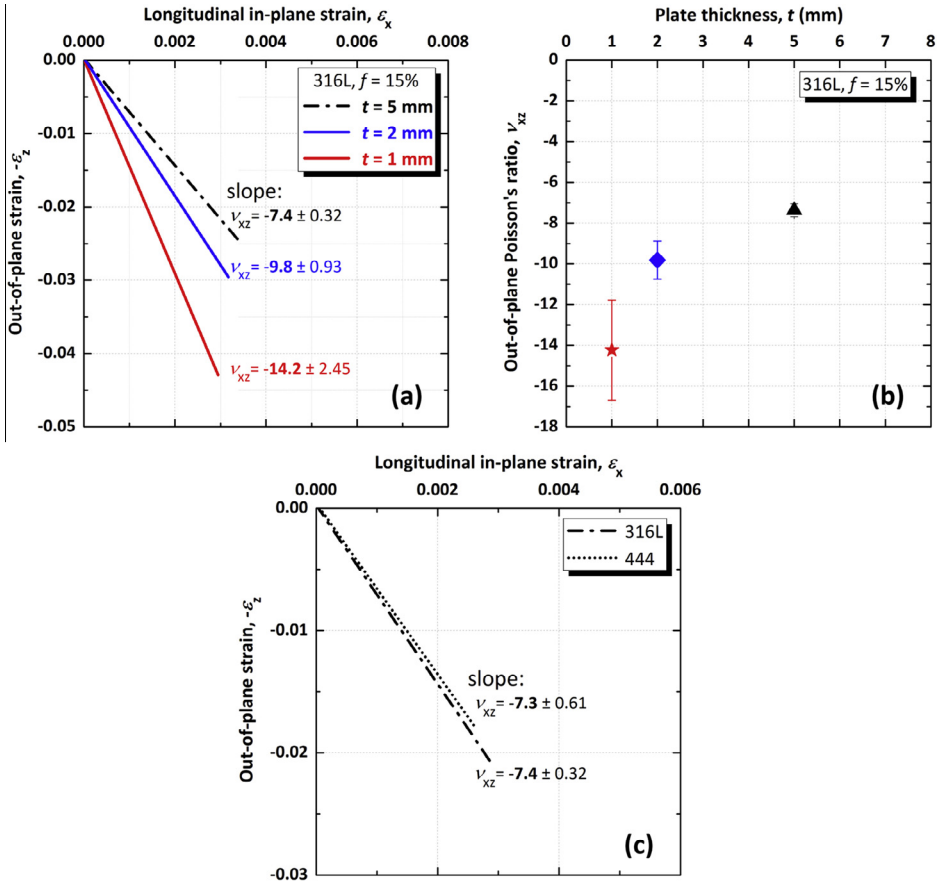

Figure 4. (a) In-plane longitudinal strain as a function of out-of-plane strain for 316L fibre networks with $f = 15\%$, with three different plate thicknesses; (b) experimental dependence on plate thickness of the out-of-plane Poisson's ratio of 316L fibre networks with $f = 15\%$; (c) in-plane longitudinal strain as a function of out-of-plane strain for 316L and 444 fibre networks with $f = 15\%$.

Figure 3b shows that the mean fibre segment inclination angles, with respect to the out-of-plane direction (z axis), are somewhat lower for lower fibre content networks, i.e. fibre segments are sitting more in-plane in the 10% networks.

A further observation is that the inter-layer bonding in these networks is weak causing the networks to continuously expand in the through-thickness direction with increasing load (beyond the elastic region), thereby resulting in intra-laminar cracking and significant through-thickness thickening [34].

In order to investigate whether the number of inter-layers, i.e. the network thickness, affects the Poisson's ratio, in-plane tensile testing was carried out using 316L networks of the same fibre volume fraction but with different plate thicknesses. Figure 4a shows the longitudinal strain ε_x versus the out-of-plane strain ε_z for 316L networks with 15% fibre volume fraction. It can be seen that the slopes, representing the out-of-plane Poisson's ratio, become more negative with decreasing plate thickness. As Figure 4b illustrates, the

Table 2. Out-of-plane Young's modulus E_z for 316L fibre networks with different fibre volume fractions, as obtained by DMA testing. Also, shown are the in-plane Young's moduli (E_x and E_y) measured using tensile testing [34]. All measurements were carried out using 5 mm thick plates.

Fibre volume fraction f (%)	Young's moduli (GPa)		
	Out-of-plane	In-plane	
	E_z	E_x	E_y
10	0.0069 ± 0.0011	1.17 ± 0.32	1.13 ± 0.06
15	0.0087 ± 0.0011	2.19 ± 0.11	2.28 ± 0.59
20	0.0094 ± 0.0006	2.51 ± 0.06	3.10 ± 0.86

auxetic effect amplifies (i.e. negative Poisson's value increases) almost exponentially as the thickness of the plate reduces from 5 mm to 1 mm. Assuming that the inter-layer bonding is not changing with network thickness, the observed trend suggests that thin plates, with less inter-layers, can expand more freely in the out-of-plane direction, leading to a more negative Poisson's value as compared to thick plates, which are more constrained by the larger number of inter-fibre layers. This suggests that weak inter-layer bonding plays a role in the auxetic response of these networks.

Table 2 shows the out-of-plane Young's modulus (E_z) of the networks obtained from DMA testing. Also, shown for comparison, are the in-plane Young's moduli (E_x and E_y) obtained from in-plane tensile testing [34]. As expected, the values are dominated by the dependence on fibre volume fraction, i.e. the Young's moduli increase with increasing fibre volume fraction. The out-of-plane modulus is approximately two orders of magnitudes lower than the corresponding in-plane values. This is unsurprising, as fibres inclined at high θ angles to the vertical will offer low resistance to vertical displacement.

In order to further verify that the auxetic behaviour arises by virtue of the network's structure and processing, a different network, made of 444 ferritic stainless steel fibres, was considered. While the sintering conditions are expected to be slightly different (because of the different fibre material), the 444 networks are processed in a similar fashion as 316L networks. However, the 444 fibres have a non-uniform cross-sectional shape (rectangular *vs* cylindrical for 316L fibre), so in practice the fibres would bend in planes in which they have relatively low moment of inertia. Figure 4c shows the longitudinal strain ε_x versus the out-of-plane strain ε_z, for both 316L and 444 networks of the same fibre volume fraction ($f = 15\%$). (Specimen dimensions and experimental parameters were the same as those used for testing 316L networks). It can be seen that similar Poisson's ratios were measured on both networks, suggesting that the out-of-plane auxetic response of the fibre networks mainly arises from the processing method.

In summary, sintered metallic fibre network mats exhibit a strong out-of-plane auxetic behaviour. The auxetic effect is attributed to fibre straightening (i.e. outward bending) in response to in-plane tensile testing. Fibre kinking is induced during processing due to the applied pressure. The results suggest that weak inter-layer bonding, high fibre content and low network thickness tend to amplify the auxetic effect.

This research was supported by the European Research Council (ERC) (Grant No. 240446). We wish to thank Dr. Kalin Dragnevski at The Laboratory for *In situ* Microscopy and Analysis (LIMA) in the Department of Engineering Science, Oxford University for the help in setting up the *in situ* DEBEN experiments.

Supplementary data associated with this article can be found, in the online version, at http://dx.doi.org/10.1016/j.scriptamat.2015.04.028.

[1] R. Lakes, Science 235 (1987) 1038.
[2] K.E. Evans, M.A. Nkansah, I.J. Hutchinson, S.C. Rogers, Nature 353 (1991) 124.
[3] R. Lakes, Adv. Mater. 5 (1993) 293.
[4] K.E. Evans, K.L. Alderson, Eng. Sci. Educ. J. 9 (2000) 148.
[5] K.E. Evans, A. Alderson, Adv. Mater. 12 (2000) 617.
[6] G.N. Greaves, A.L. Greer, R.S. Lakes, T. Rouxel, Nat. Mater. 10 (2011) 823.
[7] Y. Prawoto, Comput. Mater. Sci. 58 (2012) 140.
[8] A.E.H. Love, A Treatise on the Mathematical Theory of Elasticity, second ed., Cambridge University Press, Cambridge, 1906.
[9] D.J. Gunton, G.A. Saunders, J. Mater. Sci. 7 (1972) 1061.
[10] Y. Li, Phys. Status Solidi (A) 38 (1976) 171.
[11] R.H. Baughman, J.M. Shacklette, A.A. Zakhidov, S. Stafstrom, Nature 392 (1998) 362.
[12] Z.A.D. Lethbridge, R.I. Walton, A.S.H. Marmier, C.W. Smith, K.E. Evans, Acta Mater. 58 (2010) 6444.
[13] A. Yeganeh-Haeri, D.J. Weidner, J.B. Parise, Science 257 (1992) 650.
[14] J.N. Grima, R. Gatt, V. Zammit, J.J. Williams, K.E. Evans, A. Alderson, R.I. Walton, J. Appl. Phys. 101 (2007) 086102.
[15] R.H. Baughman, D.S. Galvao, Nature 365 (1993) 735.
[16] J.N. Grima, K.E. Evans, Chem. Commun. 36 (2000) 1531.
[17] C. He, P. Liu, P.J. McMullan, A.C. Griffin, Phys. Status Solidi (B) 242 (2005) 576.
[18] D.R. Veronda, R.A. Westmann, J. Biomech. 3 (1970) 15.
[19] C. Lees, J.F.V. Vincent, J.E. Hillerton, Bio-Med. Mater. Eng. 1 (1991) 19.
[20] R.F. Gibson, M.F. Ashby, G.S. Schajer, C.I. Robertson, Proc. R. Soc. London Ser. A 382 (1982) 25.
[21] R.F. Almgren, J. Elast. 15 (1985) 427.
[22] E.A. Friis, R.S. Lakes, J.B. Park, J. Mater. Sci. 23 (1988) 4406.
[23] D. Prall, R.S. Lakes, Int. J. Mech. Sci. 39 (1997) 305.
[24] B.D. Caddock, K.E. Evans, J. Phys. D: Appl. Phys. 22 (1989) 1877.
[25] K.L. Alderson, K.E. Evans, Polymer 33 (1992) 4435.
[26] K.E. Evans, B.D. Caddock, J. Phys. D: Appl. Phys. 22 (1989) 1883.
[27] J.N. Grima, R. Caruana-Gauci, D. Attard, R. Gatt, Proc. R. Soc. A 468 (2012) 3121.
[28] R.F. Gibson, Principles of Composite Material Mechanics, first ed., McGraw-Hill, New York, 1994.
[29] S. Jayanty, J. Crowe, L. Berhan, Phys. Status Solidi (B) 248 (2011) 73.
[30] C.T. Herakovich, J. Compos. Mater. 18 (1984) 447.
[31] J.F. Clarke, R.A. Duckett, P.J. Hine, I.J. Hutchinson, I.M. Ward, Composites 25 (1994) 863.
[32] K.E. Evans, J.P. Donoghue, K.L. Alderson, J. Compos. Mater. 38 (2004) 95.
[33] K.L. Alderson, V.R. Simkins, V.L. Coenen, P.J. Davies, A. Alderson, K.E. Evans, Phys. Status Solidi (B) 242 (2005) 509.
[34] S. Neelakantan, W. Bosbach, J. Woodhouse, A.E. Markaki, Acta Mater. 66 (2014) 326.
[35] F. Delannay, T.W. Clyne, in: J. Banhart, M.F. Ashby, N.A. Fleck (Eds.), Metal Foams and Porous Metal Structures, MIT-Verlag, 1999, pp. 293–298.
[36] M. Tatlier, L. Berhan, Phys. Status Solidi (B) 246 (2009) 2018.
[37] R.D. Bruyne, H. Schepeas, I. Lefever, R. Loufeld, in: United States Patent; Patent Number: 4983467, N.V. Bekaert S.A., Zwevegem, Belgium, 1991.